

Internal geophysics (Applied geophysics)

# An integrated study of the hydrogeology of volcanic islands using helicopter borne transient electromagnetic: Application in the Galápagos Archipelago

Esben Auken<sup>a</sup>, Sophie Violette<sup>b,\*</sup>, Noémi d'Ozouville<sup>b,c</sup>, Benoît Deffontaines<sup>d</sup>,  
Kurt I. Sørensen<sup>a</sup>, Andrea Viezzoli<sup>a</sup>, Ghislain de Marsily<sup>b,c</sup>

<sup>a</sup> University of Aarhus, HydroGeophysics Group, Department of Earth Sciences, Høegh-Gulbergs gade 2, 8000 Århus, Denmark

<sup>b</sup> UMR 7619-Sisyphé, université Pierre-et-Marie-Curie, case 105, 4, place Jussieu, 75252 Paris cedex 05, France

<sup>c</sup> CNRS, UMR 7619-Sisyphé, 75252 Paris cedex 05, France

<sup>d</sup> UMR-ISTEP, CNRS, université Pierre-et-Marie-Curie, 4, place Jussieu, 75252 Paris cedex 05, France

Received 10 October 2008; accepted after revision 1 July 2009

Available online 7 October 2009

Written on invitation of the Editorial Board

## Abstract

The hydrology of volcanic islands is poorly characterized due to their complex internal structure and challenging access. The Galápagos Islands, an isolated basaltic environment with unique ecosystems and growing anthropogenic pressure, suffer from scarcity of freshwater resources and from the lack of fundamental knowledge on their hydrology. To overcome these constraints and provide fresh water to the population, a geophysical survey and a hydroclimatologic network at watershed scale have been performed over Santa Cruz. An innovative helicopter borne transient electromagnetic method permitted a quasi-3D (an inversion scheme allowing for a 3D model description but with a local 1D forward algorithm) resistivity mapping of the massif and the identification of its hydrogeological potential. The latter is composed of a perched aquifer on the windward mountainside and a basal aquifer. Our hydroclimatologic network provided useful data records and allowed us to characterize the hydrodynamic properties of the basal aquifer. The geophysical data allow us to precise its extension. The conceptual hydrogeological model proposed for Santa Cruz confirms one of the models proposed for Le Piton de la Fournaise (Réunion Island). It has now to be confirmed with boreholes and a detailed geochemical study including noble gas analysis. **To cite this article: E. Auken et al., C. R. Geoscience 341 (2009).**

© 2009 Académie des sciences. Published by Elsevier Masson SAS. All rights reserved.

## Résumé

**Étude intégrée de l'hydrogéologie d'îles volcaniques au moyen de l'électromagnétisme transitoire hélicoptérée : application aux îles Galápagos.** L'hydrologie des édifices volcaniques est méconnue, en raison notamment de la complexité de leur structure interne. Les îles Galápagos, environnement basaltique isolé, berceau d'un écosystème unique, doivent faire face à une pression anthropique croissante, et souffrent du manque d'eau douce et de l'absence de connaissances fondamentales sur le cycle

\* Corresponding author.

E-mail addresses: [esben.auken@geo.au.dk](mailto:esben.auken@geo.au.dk) (E. Auken), [sophie.violette@upmc.fr](mailto:sophie.violette@upmc.fr) (S. Violette), [pajarobrujo@gmail.com](mailto:pajarobrujo@gmail.com) (N. d'Ozouville), [benoit.deffontaines@upmc.fr](mailto:benoit.deffontaines@upmc.fr) (B. Deffontaines), [kurt.sorensen@geo.au.dk](mailto:kurt.sorensen@geo.au.dk) (K.I. Sørensen), [andrea.viezzoli@geo.au.dk](mailto:andrea.viezzoli@geo.au.dk) (A. Viezzoli), [GDemarsily@aol.com](mailto:GDemarsily@aol.com) (G. de Marsily).

hydrologique. Pour dépasser ces contraintes et répondre aux besoins en eau, une campagne géophysique et l'équipement hydroclimatologique d'un bassin versant de l'île de Santa Cruz ont été réalisés. La méthode innovante héliportée SkyTEM a permis d'obtenir un modèle de résistivité quasi-3D (un schéma d'inversion permettant une description d'un modèle 3D, en utilisant un algorithme de calcul direct 1D local) de l'édifice et l'identification de ses potentiels hydrogéologiques. Ces derniers sont composés d'un aquifère perché, situé côte au vent, et d'un aquifère de base. Les données fournies par le réseau hydroclimatologique ont permis de caractériser les propriétés hydrodynamiques de l'aquifère de base et la géophysique a permis d'en préciser l'extension. Ainsi le modèle hydrogéologique conceptuel obtenu à Santa Cruz confirme l'un des modèles proposés pour le Piton de la Fournaise, île de la Réunion. Il doit à présent être validé par le creusement de forages et une étude géochimique détaillée incluant l'analyse des gaz rares. *Pour citer cet article : E. Auken et al., C. R. Geoscience 341 (2009).*

© 2009 Académie des sciences. Publié par Elsevier Masson SAS. Tous droits réservés.

**Keywords:** Helicopter borne geophysical survey; Groundwater; Basaltic island; Time domain electromagnetic (TDEM); Transient electromagnetic (TEM); SkyTEM; Santa Cruz Island; Galápagos Archipelago

**Mots clés :** Campagne de géophysique héliportée ; Aquifère ; Île basaltique ; Électromagnétisme en domaine temporel (TDEM) ; Électromagnétisme transitoire (TEM) ; SkyTEM ; Île de Santa Cruz ; Archipel des Galápagos

## 1. Introduction

Low relief volcanic islands often suffer from scarcity of apparent freshwater resources [8,17]. Santa Cruz, Galápagos Archipelago, is one of them. For the last two decades, its exponentially growing population (6% per year) has created an urgent need for water resource management and protection of unique and pristine ecosystems. UNESCO put them on the “Endangered World Heritage list” in June 2007. This island suffers, as do the others of the Galápagos, from difficulty of access to the field (inaccessible National Park land covers more than 70% of the 986 km<sup>2</sup> of the island), extremely limited water resource monitoring (climatology, hydrology and hydrogeology) and baseline data (topography, geophysics and geology). In this context, we are interested in learning how to overcome these constraints and improve the hydrological knowledge of this island to ensure better water resource management. The use of an indirect method, such as a geophysical survey, was therefore indispensable. In this study, we used a helicopter-borne transient electromagnetic (TEM) method, SkyTEM [13], which was flown for the first time over a volcanic terrain. Relatively few other cases of ground based TEM investigations carried out in volcanic terrain are found in the literature, though a few are reported by Albouy et al. [2] and Descloitres et al. [6]. The transient method is a natural choice because of its large depth of investigation compared to, for e.g., frequency domain methods and its low cost compared to seismic. The SkyTEM system enables fast data acquisition and is a non-intrusive method capable of penetrating to a depth of about 300 m. In addition, this method provides data over inaccessible areas and a density of soundings that is much higher than any

ground survey. The aim of applying such a method was to obtain the internal resistivity structure of the massif. In particular, we are interested in identifying low resistivity layers within the dominant high resistivity basalts. These layers could indicate water saturation, presence of clays and/or mineralization. Also the results could be used to characterize the geometry of the freshwater–saltwater interface and to identify tectonic structures such as faults. Efforts were also made to deploy a hydroclimatologic network at watershed scale as well as to use another indirect method such as photo-interpretation to support data that might validate or complement the geophysics experiment.

In this paper, we present results from the novel use of the SkyTEM method over volcanic terrains: the interpretation of the data set in terms of the hydrogeological functioning of an island. We illustrate the unique data and results over a remote volcanic insular environment, which were generated by using a state-of-the-art system through in-depth processing and constrained inversion.

## 2. Settings and methods

Fig. 1 shows the location of the Galápagos Archipelago (Ecuador), 1000 km west of the South-American coast, straddling the Equator. Here we focus on the most populated island – Santa Cruz (13,000 inhabitants and 170,000 visitors per year) that is located in the central part of the archipelago. It is a volcanic island with its highest point 855 m above sea level (a.s.l.) [11]. The oldest lavas of the island are dated to 1 to 3 Ma (million years) [5], and the most recent lavas are younger than 250,000 years to a couple of thousand years [5]. The low-lying coastal apron gradually



Fig. 1. Map of the Galápagos Archipelago, insert: Ecuador of South-America continent.

Fig. 1. Carte de l'Archipel des Galápagos, encart : position de l'Équateur au sein du continent sud-américain.

steepens to reach the summit area where the predominant feature is the alignment of volcanic cones along east–west normal faults. Detailed geological maps and stratigraphic sections do not exist due to the limited outcrop areas and the lack of boreholes. The only borehole available lies about 5 km inland, at ~160 m a.s.l. It has a depth of 160 m and reaches the water table almost at this depth. It shows a monotonous series of basalt lava flows of alkaline nature.

The hydrological year starts with the “garúa” season (fog and mist season) from June to December when an inversion layer sets in above 300 m a.s.l. The moisture-laden air from the cool south-east trade winds condenses in contact with the vegetation giving rise to humid conditions, which results in a higher hydrogeological potential on the windward mountain-side. Here, the hydrogeological potential refers to the effective rainfall, which may allow runoff and/or infiltration, the latter is able to recharge perched or basal aquifers. Heavy rainstorms occur during the hot season from January to May. Annual rainfall varies from 500 mm at the coast to 1500 mm at 630 m a.s.l. [9]. Interannual variations can be very high with years without any rainfall in the coastal areas and exceptional El Niño years when precipitation can be more than four times higher [14]. There are no perennial creeks and the groundwater potential of this island is limited to a tide-influenced brackish basal aquifer (electrical conductivity EC of water: 0.1–0.7 S/m) known through vertical faults (grietas), the deep borehole and a highland low out-flow spring (0.01–0.1 l/s) at the base of a scoria

cone. To better quantify the hydrological balance, a hydroclimatologic network was set up at the Pelican bay watershed scale (43 km<sup>2</sup>) in December 2004. Over this watershed the network is composed of three rain gauges at Charles Darwin Station, elevation 5 m, Bellavista, elevation 180 m and Cerro Croker, elevation 850 m; one runoff measurement; two probes for water level, temperature and EC measurements in the basal aquifer.

SkyTEM is a time-domain electromagnetic, helicopter-borne system designed for hydrogeophysical and environmental investigations [13]. The system in operation and the flight-line map over Santa Cruz are depicted in Figs. 2 and 3, respectively. With the SkyTEM system, more than 300 line kilometers of profile data can be produced per day. The continuous data set is acquired at an average flight speed of 40 km/h. Individual soundings are represented by an integration of 3 s of data, resulting in a data set of one sounding every 30 m along the profiles. The average spacing between two parallel flight lines was 200 m. Vertical penetration is typically in the order of 200 to 300 m depending on the medium. The system transmits two magnetic moments, a low moment (number of turns multiplied by the area multiplied by the current in the transmitter loop) for resolution of the near surface

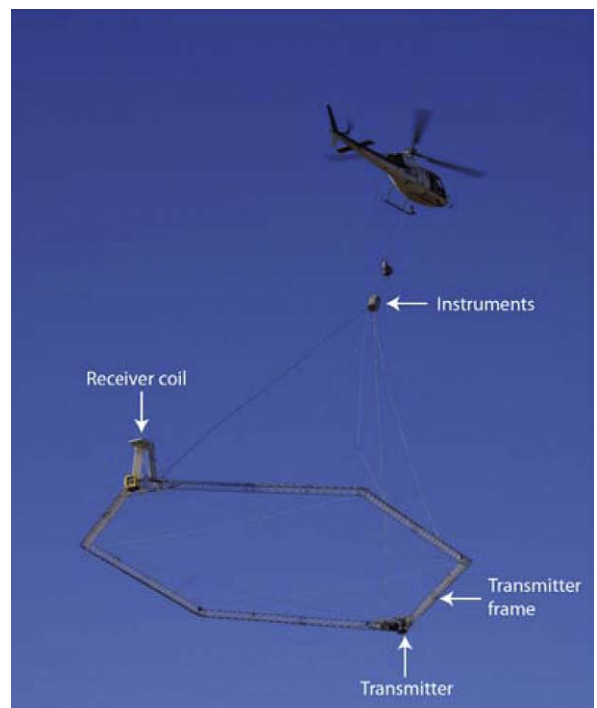


Fig. 2. SkyTEM device in operation.

Fig. 2. Système SkyTEM en opération.

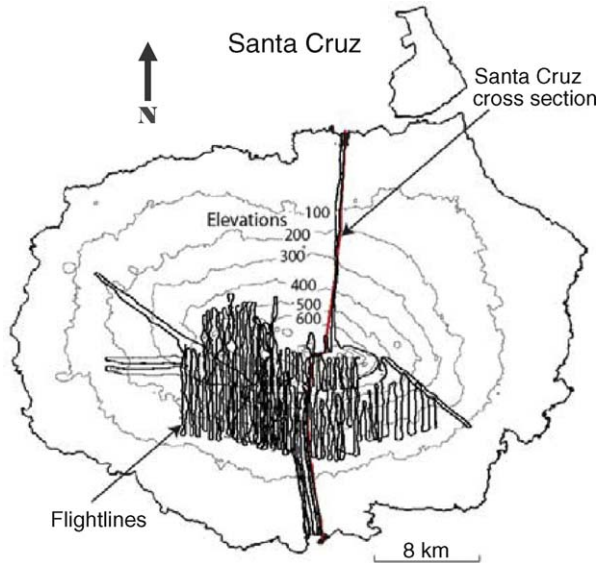


Fig. 3. Map of flight lines over Santa Cruz Island. Contour lines: elevations given as meters above sea level (a.s.l.)

Fig. 3. Carte des lignes de vol au-dessus de l'île de Santa Cruz. Isocontour : altitude en mètres au-dessus du niveau moyen des mers.

layers and a high moment for resolution of the deeper layers. Detailed information on system calibration and field procedure is given by Sørensen and Auken [13]. Processing of the data (transients and navigation data) is implemented as a module in the Aarhus Workbench: a software platform for working with geophysical, geological and GIS data. It has fully integrated modules for processing and inversion of the data, generating geophysical theme maps, and visualization in a GIS environment. To achieve maximum credibility of the models resulting from the inversion, the raw data are corrected for pitch and roll of the transmitter and receiver loops. Data are gently filtered at late times to achieve as much penetration depth as possible without compromising (too much) the lateral resolution. The different processing and inversion steps are described in Auken et al. [3,4]. In the inversion scheme, the flight height is included as an inversion parameter with a prior value and a standard deviation determined from the laser altimeters attached to the transmitter frame. The inversion of the SkyTEM data was done using the quasi 3-D spatially constrained inversion (SCI) scheme [15]. The SCI scheme has a 3D model description but uses locally a 1D forward solution. Practically speaking the local 1D models are not only constrained along the flight lines but also between the flight lines reflecting the nature of the underlying 3D geological model. Constraining the model parameters spatially enhances the resolution of model parameters (i.e., resistivities and

layer interfaces), which are not well resolved in an independent inversion. The parameters are tied together with a spatially dependent covariance.

### 3. Geophysical results and hydrogeological interpretations

On Santa Cruz the area covered by the SkyTEM investigation represents 190 km<sup>2</sup> in 6 days. Transects were prepared in order to cover the largest possible area of interest with the restriction of no flights over urban zones due to signal coupling. Most lines were focused on the windward slopes where the highest potential of finding low-resistivity layers was expected. Very importantly, preliminary data processing and inversion was carried out on a daily basis in order to best direct the survey undertaken the following day. During the post-processing of the data, automatic filters (culling noisy data) were used but because of the extreme wide range of resistivities present from seawater (1–10 ohm m) to unweathered basalts (1000–8000 ohm m) the data set also had to be partly manually processed. After processing, inversions were carried out and the resulting models verified for data fit and accuracy. Both smooth and layered inversions were carried out. An example of a sounding showing saltwater at depth is shown in Fig. 4. The 3D resistivity model was generated for the island as profiles along the flight lines (Fig. 5) and spatially averaged horizontal resistivity maps at different depths (Fig. 6). Depth rather than elevation-based maps are more representative in the volcanic insular environment as they follow the building sequence of the volcanic edifice. Layers are not horizontal as in sedimentary environments but are theoretically parallel to the slopes of the volcano. The resistivity model is obtained down to a depth of 250–300 m. The range of low to intermediate resistivity is of particular interest as it may represent actual fresh water saturated media or impermeable layers on which aquifers may form. Very low resistivity values characterize basalt saturated by saltwater encountered in the basal aquifer.

Validation of the resistivity profiles is impeded due to the lack of geological data on the sub-surface structures and borehole logs. The only deep borehole on Santa Cruz is located within a low-lying area where unweathered and unsaturated basalts are found in the entire log, except on the last half meter where the basal aquifer is reached. Nevertheless the hydroclimatic network provides useful quantitative data. The water level records in the deep borehole and the grietas provide the range of the hydraulic gradient of the basal



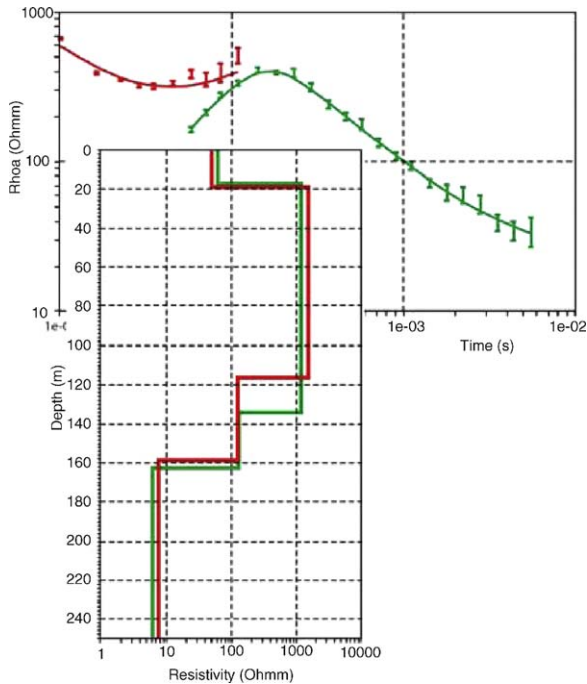


Fig. 4. a) Data sounding and forward response, b) inverted model. The low 8 ohm.m resistive layer at depth is saturated basalt with saltwater.

Fig. 4. a) Données de sondage et réponse inversée, b) modèle d'inversion. Le niveau de faible résistivité 8 ohm.m correspond à du basalte saturé en eau salée.

aquifer on the windward mountainside, i.e., 0.0001. The observed correlation between the oceanic tide signal and the water level recorded on an hourly basis, allow us to determine the diffusivity coefficient of the basal aquifer using the Ferris [7] equation ( $D = T/S$ : 50–90  $m^2/s$ ) [10]. In order to characterize the infiltration capacity of the soil at low elevations and the alterite cover in higher regions, hydraulic conductivities were measured. They range from  $1.5 \times 10^{-3}$  to  $3 \times 10^{-6}$  m/s for 150 to 394 m a.s.l., respectively [1]. In parallel, an orographic rainfall gradient of 320 to 540 mm per 100 m of elevation was recorded, together with an orographic temperature gradient of  $-0.8$  °C per 100 m of elevation. This means that the effective rainfall (the water available for the flow-infiltration and runoff) occurs above 500 m of elevation and then increase with altitude [10].

The 3D-resistivity model (Figs. 5 and 6) shows:

- 1) the north side of the island consists mainly of high resistive basalts;
- 2) a low resistivity layer is present evenly all around the island;

- 3) an intermediate resistivity range is observed for a thin superficial layer on the leeward mountain side;
- 4) a low resistivity layer at intermediate depth on the windward mountain side.

The high resistivities present in the northern part of San Cruz are consistent with the distribution of windward and leeward mountainsides of the island and the highly resistive nature of fresh unweathered basalts. The resistivity models confirmed that the weathering processes on the leeward side of the Galápagos Islands are extremely limited and therefore a very low hydrogeological potential is expected in this area. The infiltrated part of the effective rainfall, if any (no measurements are available in this leeward highland), must percolate straight down to the basal aquifer due to the high secondary permeability in the basalts via fractures.

The low-resistivity layer visible from the coast inland is a well-defined saltwater intrusion wedge. Seawater intrusion along coastal environments has been widely studied. It is a natural phenomenon governed by the difference in density between fresh water and seawater. The inversion results show that the seawater intrusion is present all around the island. The signal from the saltwater is perceptible up to an elevation of about 300 m on the northern side of the islands, and about 200 m on the southern side. The fresh water–seawater interface is found at a maximum elevation of  $-30$  m a.s.l. on the leeward mountainside (northern side) contrasting with the  $-90$  m a.s.l. on the windward side (southern side; Fig. 7) as it is recognized up to 9 km inland on both sides of the massif. Hydrogeologically, the top of the saltwater is important as a proxy for the presence of a freshwater lens. Up to 5 km inland on Santa Cruz Island (i.e., deep borehole), it is known that this freshwater lens consists mainly of brackish water. Far inland (at 9 km) one can predict that the water will become fresher. As yet, our results do not permit detection of the presence of fresh or brackish water on top of the seawater, but this may be achieved by careful reprocessing of the geophysical data. However the different hydraulic gradients between the two mountain sides deduced from the gradient of the fresh water–saltwater interface is consistent with what is known about the available quantity of effective rainfall on both sides. We infer that this quantity is much smaller on the leeward side than in the highland of the windward side (almost zero on the leeward side compared to  $\sim 400$  mm per year on the windward side). The very low resistivity signature also reveals the good permeability of the

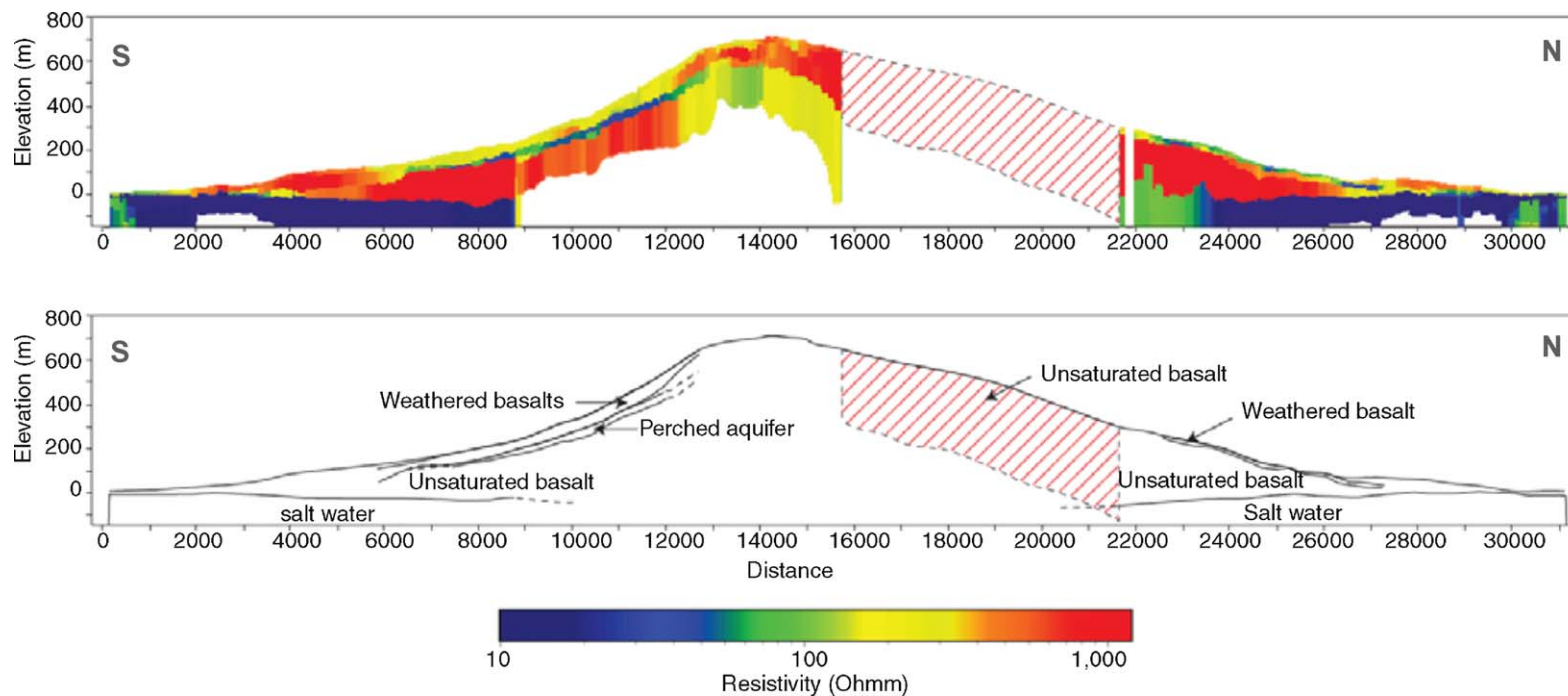
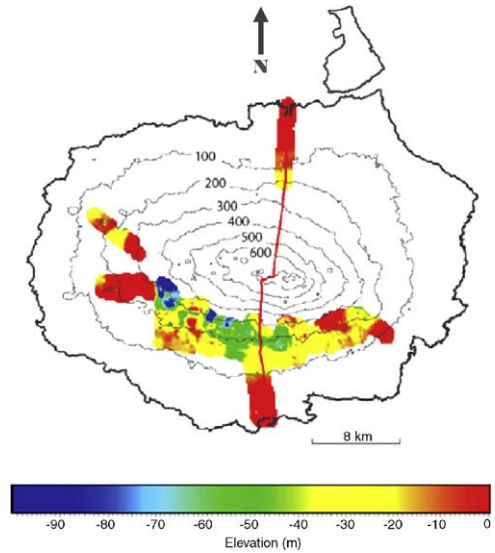
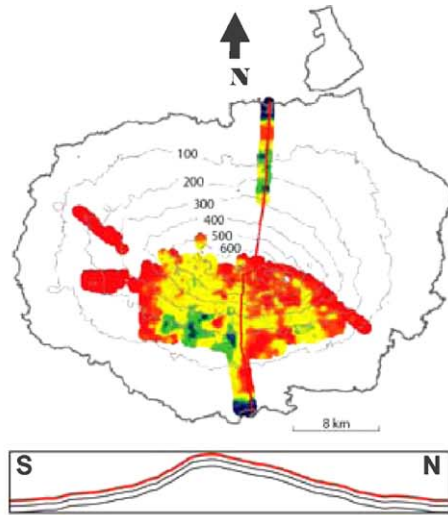
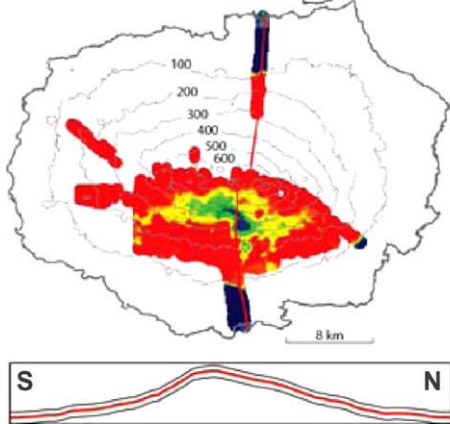


Fig. 5. a) Resistivity profile along a south–north cross-section, b) hydrogeological interpretation scheme showing the potential hydrogeological units. The red hatching shows a portion of the profile where the signal level was very low, indicating thick, very resistive layers, i.e., unsaturated basalts.

Fig. 5. a) Profil de résistivité le long d'une coupe sud–nord, b) schéma interprété montrant les différentes unités hydrogéologiques. Les hachures en rouge montrent la portion du profil où le signal était très faible, indiquant un niveau épais très résistant, i.e., basalte non saturé.



b) Average resistivity 80–100 m



c) Average resistivity 160–200 m

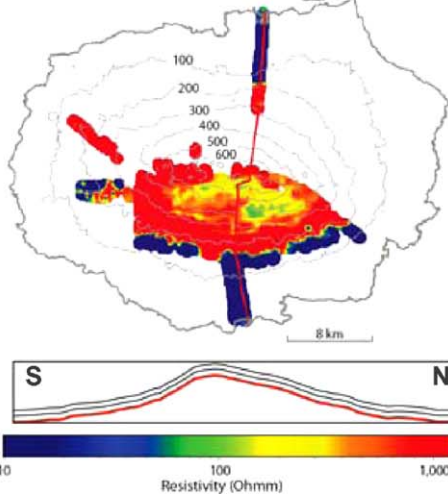


Fig. 7. Map of the depth of the fresh water–saltwater interface derived from the 3D-resistivity model of Santa Cruz. Elevation gave as meters above sea level (a.s.l.)

Fig. 7. Carte représentant la profondeur de l’interface eau douce–eau salée, obtenue à partir du modèle de résistivité 3D de Santa Cruz. Altitude exprimée en mètres au-dessus du niveau moyen des mers.

fractured basalt, according with our hydrodynamic parameter estimates (Section 2).

The intermediate resistivity range for a thin superficial layer on the leeward mountainside (Fig. 5) corresponds to a thin weathered layer, inferred to be a colluvial deposit. The low resistivity layer at intermediate depth (i.e., 80–100 m, Fig. 6) on the windward mountainside may correspond to a continuous perched aquifer [12]. In fact, the measured resistivities (50–130 ohm.m) are in the range of those given in the literature for fresh water-saturated volcanic formations. The layer covers an area of 50 km<sup>2</sup> and slopes parallel to the topography on the north-south direction (Fig. 5) and gently to the East of the island in the east-west direction (Fig. 6). Its thickness is 80 m up slope and reduces to 10 m down slope. It is buried approximately 100 m deep and does not outcrop. Everywhere along the profiles it ends abruptly without obvious physical contact; there is no contact either with the topography, or with the basal aquifer, which lies much deeper. This means two things: first, that

Fig. 6. Average resistivity maps at different depth below ground level: a) 0–20 m, b) 80–100 m, c) 160–200 m. The profiles underneath the maps illustrate the different depth slices.

Fig. 6. Carte de résistivité moyenne à différentes profondeurs sous la surface du sol : a) 0–20 m, b) 80–100 m, c) 160–200 m. Les profils sous les cartes indiquent les différentes tranches de profondeur.

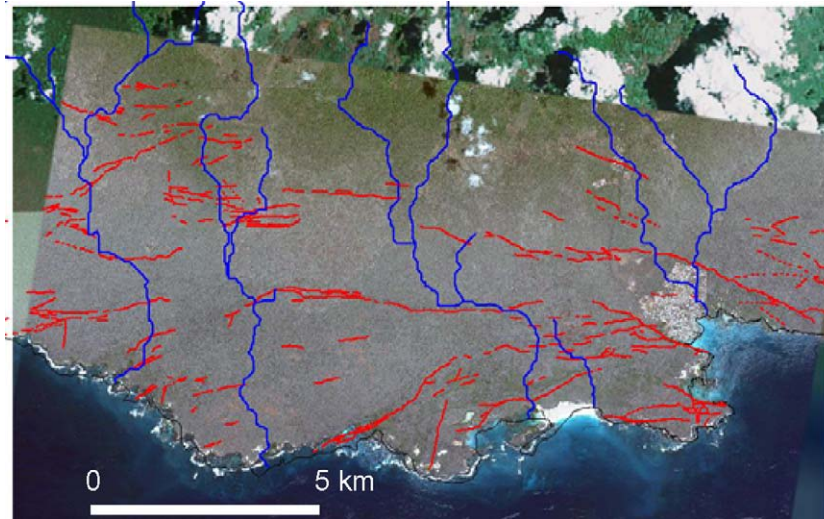


Fig. 8. Map of fractures (in red) and surface drainage network (in blue) extracted manually from a GoogleEarth<sup>®</sup> mosaic, southern windward side of Santa Cruz.

Fig. 8. Carte de fracturation (en rouge) et du réseau de drainage (en bleu) extrait manuellement d'une mosaïque éditée par GoogleEarth<sup>®</sup>, versant sud au vent de Santa Cruz.

groundwater flow has no chance of reaching the surface and feed a spring; second, the groundwater flows in line with the higher slope of the layer and then meets some vertical fractures or faults which ensure recharge to the basal aquifer. The hydrodynamic connection between the two aquifers (perched and basal) is inferred to be indirect through vertical joints and faults. Such structures have been recognized by aerial photograph interpretation and in the field (Fig. 8). The perched aquifer is either composed of colluvial interbedded lava flow deposit or fractured basalt lava flow covering a pyroclastic deposit during the shield-building phase of the volcanism. These deposits are easily weathered to clays and could consist of an impermeable layer, especially if they had been covered by hot lava of subsequent eruptions and “baked” to form “red-layers” as has been observed on other volcanic islands around the world and in the archipelago. The TEM measurements cannot resolve such a thin layer, expected to be 5 to 10 m thick.

#### 4. Discussion and conclusions

The use of the SkyTEM method over the Galápagos archipelago brings unprecedented results to the scientific community: geophysics, hydrogeology, volcanology, geomorphology and structural geology. Carefully processing of the unbiased data and subsequent application, for the first time, of the SCI inversion scheme have resulted in images with as high a lateral

and vertical resolution of the subsurface geology as can be achieved from any electromagnetic system, ground-based or helicopter-borne. The vertical depth of penetration with the applied system [3] is between 250 and 300 m depending on the overall resistivity of the subsurface and on the natural noise background level.

The unique data generated for the Galápagos Islands suggest the potential for understanding the internal structure of other oceanic volcanic islands. Ideally log data from boreholes are needed to validate the 3D-resistivity model. The study has allowed further advances in the hydrogeological conceptual model of the Galápagos Islands. Results show that the volcanic islands of the Galápagos Archipelago are subject to a very strong dichotomy between the southern and northern slopes. All hydrogeological potential is concentrated on the southern slopes as expected at the start of the study. The saltwater interface is continuously present around the island, but closer processing and inversion of data is still necessary in order to detect the freshwater lens above the saltwater and to determine the influence of local hydrogeological conditions such as impermeable barriers or preferential flow paths through open faults. A potential perched aquifer layer on Santa Cruz has been identified and characterized. This feature is in good agreement with the hydrogeological model proposed for Piton de la Fournaise, Réunion Island by Violette et al. [16].



## Acknowledgments

The authors thank the following institutions and foundations for funding: Fondation de France, Fondation Entreprise Véolia Environnement, Fondation Schlumberger-SEED, Naturalia et Biologia, université Pierre-et-Marie-Curie, European Space Agency, Chancellerie des universités de l'Académie de Paris, Municipality of Santa Cruz and BID-UGAFIP. Also we thank our local collaborators for making every possible effort to make this fieldwork possible: Galápagos National Park Service, Charles Darwin Foundation, Galápagos National Institute, Municipality of Santa Cruz. Thanks to all the field crew – pilot, technician from Aviandina and AeroMaster Airways, Susana Avila in the Wildaid office, the other field helpers and taxi drivers. Very special thanks to Godfrey Merlen, Lars Rasmussen and Jan Steen Jørgensen.

## References

- [1] M. Adelinet, J. Fortin, N. d'Ozouville, S. Violette, The relationship between hydrodynamic properties and weathering of soils derived from volcanic rocks – Galápagos Islands (Ecuador), *Environ. Geol.* 56 (2008) 45–58, doi:10.1007/s00254-007-1138-3.
- [2] Y. Albouy, P. Andrieux, G. Rakotondrasoana, M. Ritz, M. Descloitres, J.-L. Join, E. Rasolomanano, Mapping coastal aquifers by joint inversion of DC and TEM sounding, three case histories, *Groundwater* 39 (2001) 87–97.
- [3] E. Auken, N. Foged, J.A. Westergaard, A.V. Christiansen, K.I. Sørensen, Processing, inversion, and management of SkyTEM data for groundwater investigations, AEM workshop, BGR Hannover, Germany, 2006.
- [4] E. Auken, J.A. Westergaard, A.V. Christiansen, K.I. Sørensen, Processing and inversion of SkyTEM data for high resolution hydrogeophysical surveys, ASEG, Perth, western Australia, 2007.
- [5] C.S. Bow, Geology and petrogenesis of lavas from Floreana and Santa Cruz Islands, Galapagos Archipelago, Ph.D. Thesis Univ. Oreg., 1979, 350 p.
- [6] M. Descloitres, M. Ritz, B. Robineau, M. Courteaud, Electrical structure beneath the eastern collapsed flank of Piton de la Fournaise volcano, Reunion Island: Implications for the quest of groundwater, *Water Resour. Res.* 33 (1997) 13–19.
- [7] J. Ferris, Cyclic fluctuations of water levels as a basis for determining aquifer transmissibility, 33-2, IAHS Publication, Wallingford, UK, 1951, pp. 148–155.
- [8] C. Herrera, E. Custodio, Conceptual hydrogeological model of volcanic Easter Island (Chile) after chemical and isotopic surveys, *Hydrogeol. J.* 16 (2008) 1329–1348, doi:10.1007/s10040-008-316-z.
- [9] C. Huttel, Vegetación en Coladas de Lava, Islas Galápagos, Ecuador, Fundación Charles Darwin (Eds), Quito, 1995.
- [10] N. d'Ozouville, Étude du fonctionnement hydrologique dans les îles Galápagos : caractérisation d'un milieu volcanique insulaire et préalable à la gestion de la ressource. Ph.D. Thesis, Univ. Pierre-et-Marie-Curie, France, 2007, 471 p.
- [11] N. d'Ozouville, B. Deffontaines, J. Benveniste, U. Wegmuller, S. Violette, G. de Marsily, DEM generation using ASAR (ENVISAT) for addressing the lack of freshwater ecosystems management, Santa Cruz Island, Galápagos – Special issue on Monitoring Freshwater Ecosystems, *Remote Sensing Environ.* 112 (2008) 4131–4147, doi:10.1016/j.rse.2008.02.017.
- [12] N. d'Ozouville, E. Auken, K. Sørensen, S. Violette, G. de Marsily, B. Deffontaines, G. Merlen, Extensive perched aquifer and structural implications revealed by 3D resistivity mapping in Galápagos volcano, *Earth Planet Sci. Lett.* 269 (2008) 517–522, doi:10.1016/j.epsl.2008.03.011.
- [13] K.I. Sørensen, E. Auken, SkyTEM – A new high-resolution helicopter transient electromagnetic system, *Explor. Geophys.* 35 (2004) 191–199.
- [14] H. Snell, S. Rea, The 1997–1998 El Niño in Galápagos: Can 34 years of data estimate 120 years of pattern? *Not. Galapagos* 60 (1999) 11–20.
- [15] A. Viezzoli, A.V. Christiansen, E. Auken, K. Sørensen, Quasi-3D modeling of airborne TEM data by spatially constrained inversion, *Geophysics* 73 (2008) F105–F113, doi:10.1190/1.2895521.
- [16] S. Violette, E. Ledoux, P. Goblet, J.-P. Carbonnel, Hydrologic and thermal modelling of an active volcano: the Piton de la Fournaise, La Réunion Island, *J. Hydrol.* 191 (1997) 37–63.
- [17] J.H. Won, J.W. Kim, G.W. Koh, J.Y. Lee, Evaluation of hydrogeological characteristics in Jeju Island, Korea, *Geosci. J.* 9–1 (2005) 33–46.